Systematics of low-lying state transition probabilities and excitation energies in the region $30 \leqslant Z \leqslant 38$ and $30 \leqslant N \leqslant 50$

S. L. Rice, Y. Y. Sharon, N. Benczer-Koller, G. J. Kumbartzki, and L. Zamick
Department of Physics and Astronomy, Rutgers University, New Brunswick, New Jersey 08903, USA
(Received 27 September 2013; published 31 October 2013)

Background: Single-particle and collective modes of nuclear excitation compete in the isotopes of the elements $_{30}$Zn, $_{32}$Ge, $_{34}$Se, $_{36}$Kr, and $_{38}$Sr.
Purpose: To study the factors which determine the onset of collectivity in this region.
Methods: Data obtained from National Nuclear Data Center compilations supplemented by recent measurements of excitation energies and $B(E2)$ reduced transition probabilities between the low-lying states in these elements were examined. The data were analyzed as a function of the neutron number N as well as the parameter $P = N_pN_n/(N_p + N_n)$ related to the number of valence protons and neutrons, N_p and N_n, in the $28 \leqslant Z, N \leqslant 50$ shell.
Results: The systematics of the data show variations ranging from mostly single-particle to collective excitations.
Conclusions: Collectivity sets in when the number of both protons and neutrons lie near the middle of the shell $30 \leqslant Z, N \leqslant 50$. Backbends appear in the data showing that particles and holes in the major shell behave differently. The 2_2^+ states exhibit single particle behavior. The transition probabilities of the 2_2^+ states in the Kr isotopes differ significantly from the systematics.

DOI: 10.1103/PhysRevC.88.044334 PACS number(s): 21.10.−k, 23.20.Lv, 27.50.+e

I. INTRODUCTION

The even-even nuclei with $30 \leqslant Z \leqslant 38$ are of interest for several reasons. For each element—$_{30}$Zn, $_{32}$Ge, $_{34}$Se, $_{36}$Kr, and $_{38}$Sr—there exists a long isotopic chain of nuclei, stable and radioactive. Thus, the variation of the nuclear properties for nuclei along each isotopic chain sheds light on how the structure evolves with the increase in N. On the other hand, comparing isotones from different chains provides information on how the nuclear properties change with Z.

From the shell model perspective, the nuclei examined in this paper have atomic numbers Z that lie in the first half of the $28 \leqslant Z \leqslant 50$ shell, while their number of neutrons, N, spans most of the $28 < N \leqslant 50$ shell. Hence it is rare for the nuclei in the region of interest to have both proton and neutron numbers lying simultaneously in the middle of the shell. This observation is expected to have implications for the possible onset of collectivity in this region.

The nuclear properties which are examined in this paper are the level excitation energies and the electric quadrupole reduced transition probabilities $B(E2)$'s. The magnetic moments have been considered in earlier papers [1–7] and references therein. The data that are presented in this paper were collected almost entirely from the National Nuclear Data Center (NNDC) [8] compilations, with a number of additions and corrections from published but unevaluated data [9–19].

II. DATA PRESENTATION

The conditions for the onset of collectivity in the region of interest are best displayed by the reduced electric quadrupole transition probabilities $B(E2; 2_1^+ \rightarrow 0_1^+)$.

The relevant data for each nucleus are plotted in Fig. 1 against N. The data for each element are connected by a solid line highlighting isotopic systematics in the $B(E2; 2_1^+ \rightarrow 0_1^+)$ values.

All the isotopic curves have their maxima around $N = 38$ to 42. Furthermore, the largest $B(E2; 2_1^+ \rightarrow 0_1^+)$ values occur in the Sr and Kr isotopes. Clearly, the data for Sr and Kr at $N \sim 38$ to 42 do not exhibit single-particle behavior which would predict minima instead of maxima in the $B(E2)$ values.

Figure 1 suggests that the collectivity increases when the numbers of both protons and neutrons are near the middle of the shell. Therefore the $B(E2; 2_1^+ \rightarrow 0_1^+)$ data were plotted in Fig. 2 against the factor $P = NpNn/(Np + Nn)$, described in Refs. [20,21]. Here N_p and N_n are, respectively, the number of valence protons or proton holes and valence neutrons or neutron holes counted from the magic numbers 28 and 50. The P factor represents the average number of proton-neutron pairs per valence nucleon. It thus provides an indication of the strength of the isospin $T = 0$ proton-neutron interaction which is responsible for observed increases in collectivity.

When the $B(E2; 2_1^+ \rightarrow 0_1^+)$ data are plotted against P the picture simplifies greatly. The isotopic curves coalesce. The overall magnitude of the $B(E2)$'s increases with P. However, the $B(E2)$'s and as shown below, the excitation energies as well, of isotopes with the same P bifurcate into two distinct curves exhibiting a pronounced "backbend." The degeneracy in P comes about from the procedure whereby the number of valence neutrons are counted in the first half of the shell while the number of neutron holes are counted in the second half of the shell. These backbends could be related to subshell details within the $28 \leqslant N \leqslant 50$ major shell, to the possible orbit-dependence of the $T = 0$ p-n interaction, or to shifts in the single-particle energies as N increases [22]. In the same reference, it is suggested that collective effects set in when $P \sim 4$ to 5 and deformation sets in when $P \geqslant 5$.

Similar analyses were carried out for the $B(E2; 4_1^+ \rightarrow 2_1^+)$ data in Figs. 3 and 4. While there are fewer data, the same general picture emerges. When the data are plotted against N, distinct isotopic curves with maxima at $N = 38$ to 42 are obtained. The isotopic curves again coalesce when plotted against P.

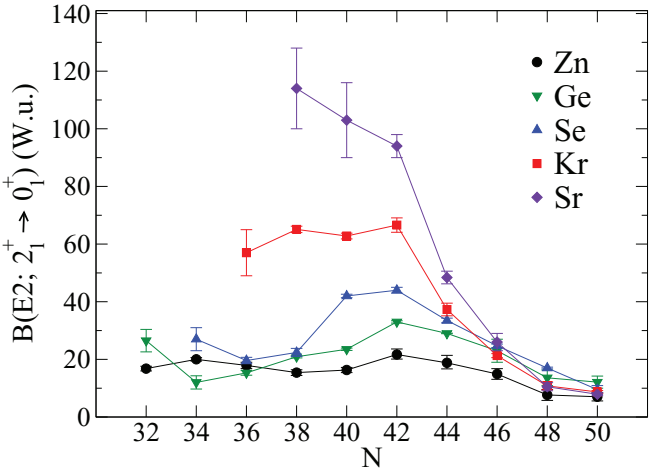

FIG. 1. (Color online) $B(E2; 2_1^+ \rightarrow 0_1^+)$'s plotted against the neutron number N. This figure is an update of Fig. 1 in Ref. [3].

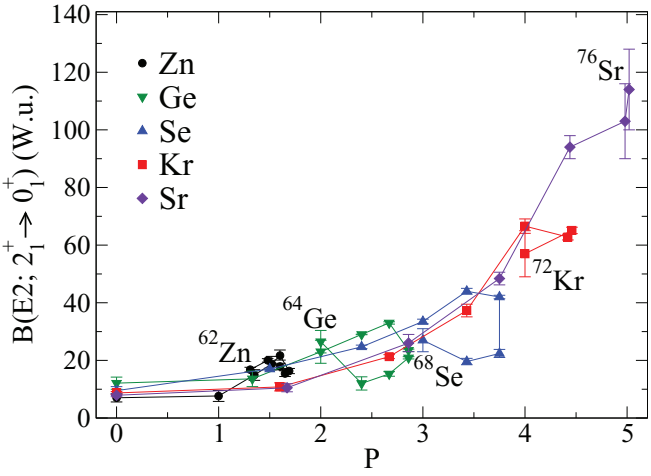

FIG. 2. (Color online) $B(E2; 2_1^+ \rightarrow 0_1^+)$'s plotted against the P factor. The lightest element in a chain is identified for each isotopic sequence.

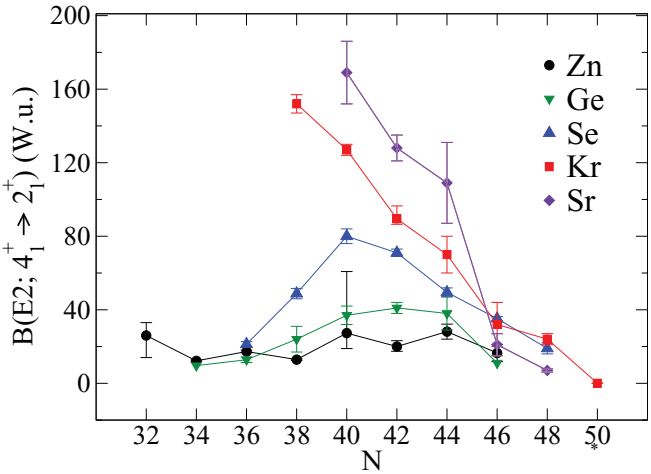

FIG. 3. (Color online) $B(E2; 4_1^+ \rightarrow 2_1^+)$'s plotted against N.

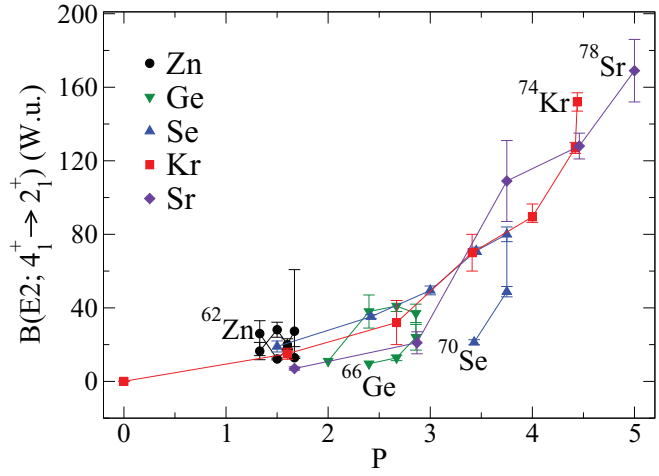

FIG. 4. (Color online) $B(E2; 4_1^+ \rightarrow 2_1^+)$'s plotted against P.

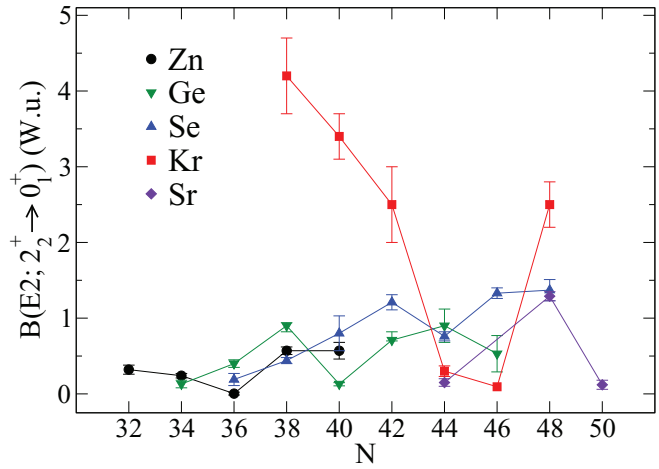

FIG. 5. (Color online) $B(E2; 2_2^+ \rightarrow 0_1^+)$'s plotted against N.

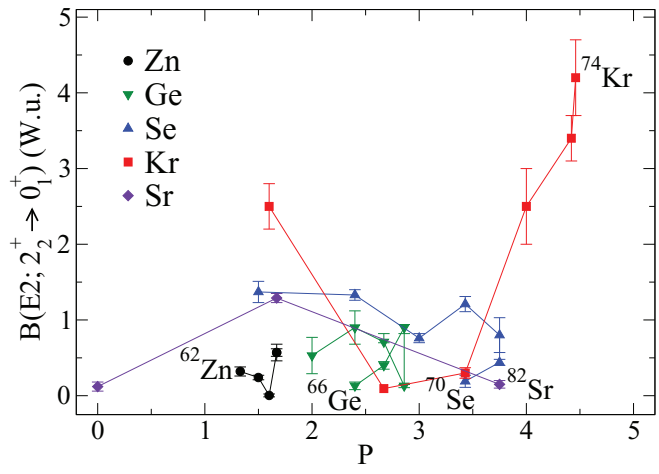

FIG. 6. (Color online) $B(E2; 2_2^+ \rightarrow 0_1^+)$'s plotted against P.

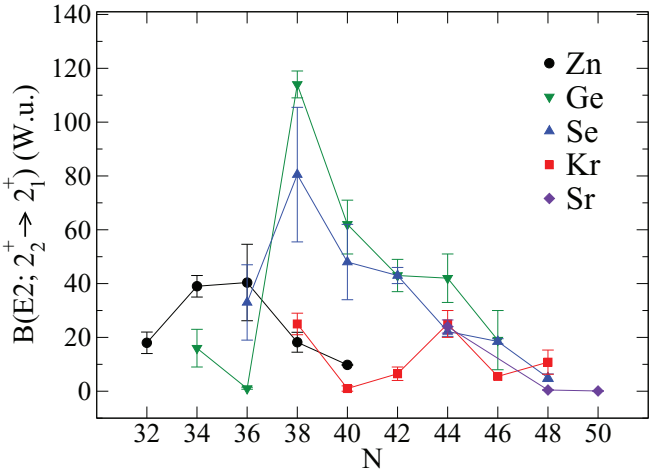

FIG. 7. (Color online) $B(E2; 2_2^+ \rightarrow 2_1^+)$'s plotted against N.

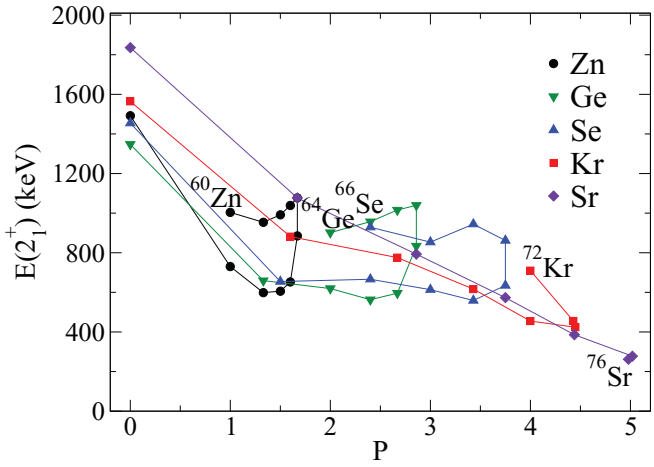

FIG. 10. (Color online) $E(2_1^+)$'s plotted against P.

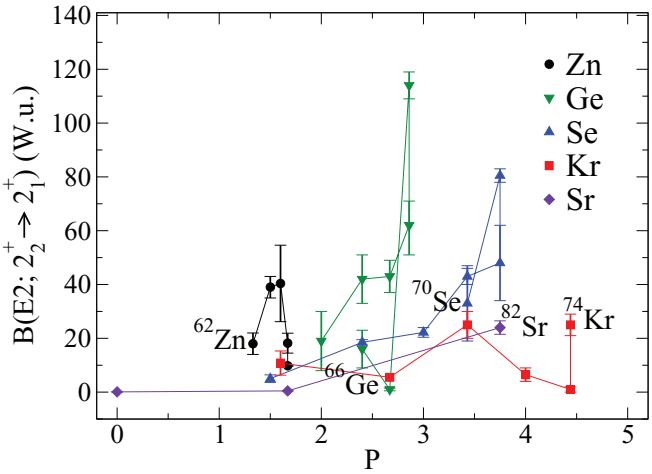

FIG. 8. (Color online) $B(E2; 2_2^+ \rightarrow 2_1^+)$'s plotted against P.

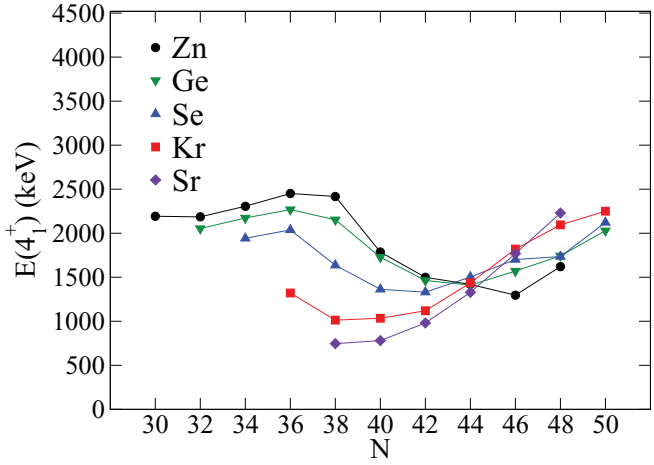

FIG. 11. (Color online) $E(4_1^+)$'s plotted against N.

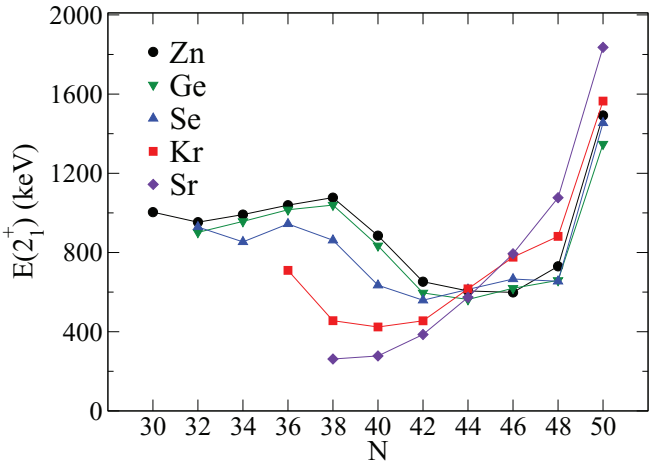

FIG. 9. (Color online) $E(2_1^+)$'s plotted against N.

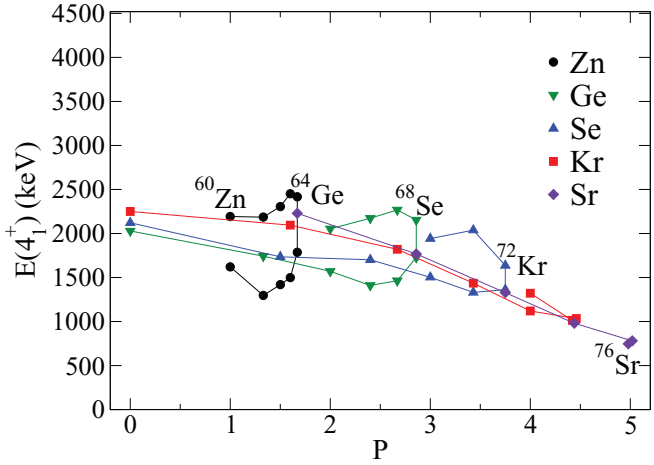

FIG. 12. (Color online) $E(4_1^+)$'s plotted against P.

To complete the presentation, the $B(E2)$ values corresponding to the decay of the 2_2^+ state to the 0_1^+ and 2_1^+ are presented in Figs. 5–8.

A key point is that the range of the values of the $B(E2; 2_2^+ \rightarrow 0_1^+)$'s is under 5 W.u. Thus, overall, these values are much smaller than the $B(E2; 2_1^+ \rightarrow 0_1^+)$ values. In the vibrational model these small values can be explained by the fact that the $2_2^+ \rightarrow 0_1^+$ transition is a forbidden two-phonon transition. In the rotational model it would be an interband, rather than an intraband, transition. A point of concern is the large divergence of the Kr isotopes in Figs. 5 and 6 from the rest of the data which could be a result of either erroneous data or a structure effect. The $B(E2; 2_2^+ \rightarrow 2_1^+)$ is generally larger than the $B(E2; 2_1^+ \rightarrow 0_1^+)$, as expected in the vibrational model.

The same presentation was extended to the excitation energies $E(2_1^+)$and $E(4_1^+)$ in Figs. 9–12. The isotopic curves for Zn and Ge in Fig. 9 almost coincide. The curve for Se is similar to them, though somewhat lower for $N \leqslant 42$. In these cases the excitation energy drops from $N = 38$ to $N = 42$ and then more or less stays flat as N increases further. However, at the magic number $N = 50$, for all the elements in Fig. 9, the $E(2_1^+)$ values are much higher. On the other hand, for Kr and Sr the excitation energies are lowest for $N = 38$ to 42, indicating more collectivity when both N and Z are near the middle of the shell, and then increase markedly with increasing N. In Fig. 10, where the same data are plotted against P, the overall trend shows a decrease of $E(2_1^+)$ as P increases. The isotopic curves coalesce less than was the case for the $B(E2)$'s, but the "backbending" behavior is more prominent than was the case for the $B(E2)$'s. The backbend effect is at its onset in the Kr isotopes; the Sr isotopes do not yet show the effect.

In order to obtain a further perspective on the collectivity of these nuclei the excitation-energy ratio $E(4_1^+)/E(2_1^+)$ is presented in Figs. 13 and 14. In a pure vibrational picture this ratio would be expected to be 2 while in a pure rotational picture it would be 3.33. When the data are plotted against N in Fig. 13, most of the ratios lie between about 2 and 2.5. The point for ^{86}Kr is low, at 1.5, an anomaly that could be associated with the 50 neutrons forming a closed shell. The Sr isotopes do not seem to follow the general pattern.

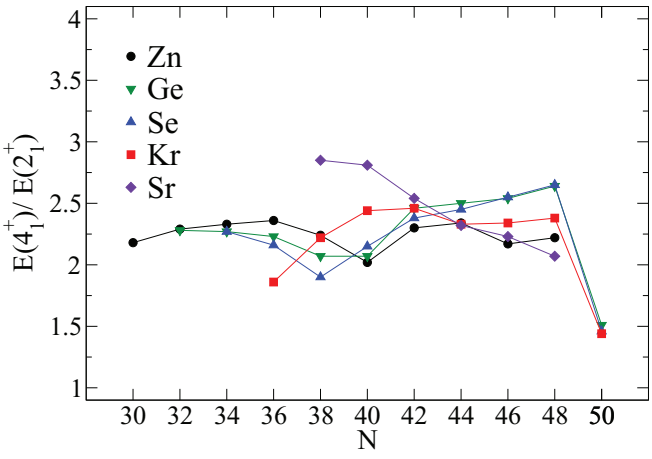

FIG. 13. (Color online) Ratio $\frac{E(4_1^+)}{E(2_1^+)}$ plotted against N.

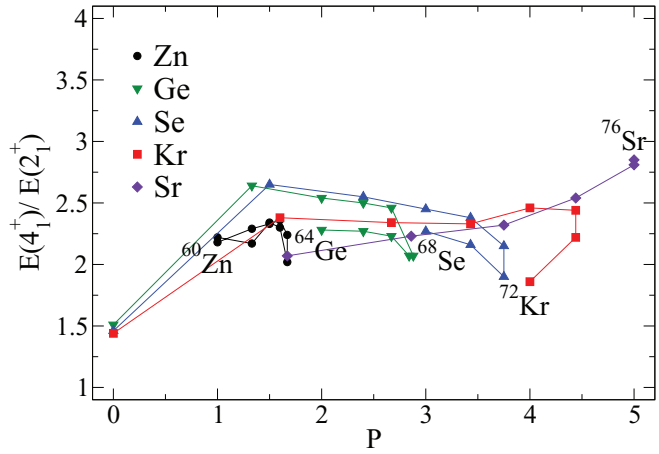

FIG. 14. (Color online) Ratio $\frac{E(4_1^+)}{E(2_1^+)}$ plotted against P.

None of the nuclei under consideration are close to being rotational. This result can be understood when the excitation-energy ratio is plotted against P in Fig. 14. The largest value of P is 5 for ^{76}Sr and ^{78}Sr. However, as is noted in Ref. [22], it is typically only for $P > 5$ that the deformation-driving $T = 0$ p-n interaction begins to dominate the spherical-driving like-nucleon pairing interaction.

III. CONCLUSIONS

The results of the present investigations confirmed that in the region of interest, for collectivity to set in, the numbers of both protons and neutrons need to be near the middle of both the $Z, N = 28$ to 50 shells.

In the study of the transition to collectivity, the use of the P factor provides a useful indicator. In the data analysis in terms of P, backbends occur in the systematics because of differences in the values of the nuclear properties for isotopes with equal numbers of neutrons or neutron holes (hence same P) in the $28 \leqslant N \leqslant 50$ shell.

The data analysis indicates that throughout the entire region the $B(E2)$ values corresponding to the $2_2^+ \rightarrow 0_1^+$ transitions are almost always considerably smaller than the $B(E2)$ values corresponding to the $2_1^+ \rightarrow 0_1^+$ and the $4_1^+ \rightarrow 2_1^+$ transitions.

Some data, in particular the transition probabilities from the 2_2^+ states in the Kr isotopes, deviate significantly from the general trends. These anomalies could be due to different structures for these isotopes or to erroneous measurements.

There are now considerable new data in the region of $30 \leqslant Z \leqslant 38$ and $30 \leqslant N \leqslant 50$ to support a critical theoretical examination of the competition between single-particle and collective modes of excitations.

ACKNOWLEDGMENTS

Y.Y.S. is grateful for a R&PD grant from Stockton College, NJ. This work was supported by the National Science Foundation.

[1] D. Mücher, G. Gürdal, K.-H. Speidel, G. J. Kumbartzki, N. Benczer-Koller, S. J. Q. Robinson, Y. Y. Sharon, L. Zamick, A. F. Lisetskiy, R. J. Casperson *et al.*, Phys. Rev. C **79**, 054310 (2009).

[2] J. Leske, K.-H. Speidel, S. Schielke, J. Gerber, P. Maier-Komor, T. Engeland, and M. Hjorth-Jensen, Phys. Rev. C **72**, 044301 (2005).

[3] G. Gürdal, E. A. Stefanova, P. Boutachkov, D. A. Torres, G. J. Kumbartzki, N. Benczer-Koller, Y. Y. Sharon, L. Zamick, S. J. Q. Robinson, T. Ahn *et al.*, Phys. Rev. C **88**, 014301 (2013).

[4] K.-H. Speidel, N. Benczer-Koller, G. Kumbartzki, C. Barton, A. Gelberg, J. Holden, G. Jakob, N. Matt, R. H. Mayer, M. Satteson *et al.*, Phys. Rev. C **57**, 2181 (1998).

[5] T. J. Mertzimekis, N. Benczer-Koller, J. Holden, G. Jakob, G. Kumbartzki, K.-H. Speidel, R. Ernst, A. Macchiavelli, M. McMahan, L. Phair *et al.*, Phys. Rev. C **64**, 024314 (2001).

[6] G. Kumbartzki, J. R. Cooper, N. Benczer-Koller, K. Hiles, T. J. Mertzimekis, M. J. Taylor, K.-H. Speidel, P. Maier-Komor, L. Bernstein, M. A. McMahan *et al.*, Phys. Lett. B **591**, 213 (2004).

[7] G. J. Kumbartzki, K.-H. Speidel, N. Benczer-Koller, D. A. Torres, Y. Y. Sharon, L. Zamick, S. J. Q. Robinson, P. Maier-Komor, T. Ahn, V. Anagnostatou *et al.*, Phys. Rev. C **85**, 044322 (2012).

[8] Evaluated Nuclear Structure Data File (ENSDF) http://www.nndc.bnl.gov/nndc/ensdf/.

[9] J. V. de Walle, F. Aksouh, T. Behrens, V. Bildstein, A. Blazhev, J. Cederkäll, E. Clément, T. E. Cocolios, T. Davinson, P. Delahaye *et al.*, Phys. Rev. C **79**, 014309 (2009).

[10] A. Gade, T. Baugher, D. Bazin, B. A. Brown, C. M. Campbell, T. Glasmacher, G. F. Grinyer, T. Honma, S. McDaniel, R. Meharchand *et al.*, Phys. Rev. C **81**, 064326 (2010).

[11] K. Starosta, A. Dewald, A. Dunomes, P. Adrich, T. Amthor, A. M. Baumann, D. Bazin, M. Bowen, B. A. Brown, A. Chester, A. Gade *et al.*, Phys. Rev. Lett. **99**, 042503 (2007).

[12] J. Ljungvall, A. Görgen, M. Girod, J.-P. Delaroche, A. Dewald, C. Dossat, E. Farnea, W. Korten, B. Melon, R. Menegazzo *et al.*, Phys. Rev. Lett. **100**, 102502 (2008).

[13] A. Osa, T. Czosnyka, Y. Utsuno, T. Mizusaki, Y. Toh, M. Oshima, M. Koizumi, Y. Hatsukawa, J. Katakura, T. Hayakawa *et al.*, Phys. Lett. B **546**, 48 (2002).

[14] E. Clément, A. Görgen, W. Korten, E. Bouchez, A. Chatillon, J. P. Delaroche, M. Girod, H. Goutte, A. Hürstel, Y. Le Coz *et al.*, Phys. Rev. C **75**, 054313 (2007).

[15] F. Becker, A. Petrovic, J. Iwanicki, N. Amzal, W. Korten, K. Hauschild, A. Hurstel, C. Theisen, P. A. Butler, R. A. Cunnigham *et al.*, Nucl. Phys. A **770**, 107 (2006).

[16] A. Lemasson, H. Iwasaki, G. Morse, D. Bazin, T. Baugher, J. S. Berryman, A. Dewald, C. Fransen, A. Gade, S. McDaniel *et al.*, Phys. Rev. C **85**, 041303(R) (2012).

[17] C. Louchart, A. Obertelli, A. Görgen, W. Korten, D. Bazzacco, B. Birkenbach, B. Bruyneel, E. Clément, P. J. Coleman-Smith, L. Corradi *et al.*, Phys. Rev. C **87**, 054302 (2013).

[18] M. Koizumi, A. Seki, Y. Toh, A. Osa, Y. Utsuno, A. Kimura, M. Oshina, T. Hayakawa, Y. Hatsuklawa, J. Katakura *et al.*, Nucl. Phys. A **730**, 46 (2004).

[19] K. Moschner, K.-H. Speidel, J. Leske, C. Bauer, C. Bernards, L. Bettermann, M. Honma, T. Möller, P. Maier-Komor, and D. Mücher, Phys. Rev. C **82**, 014301 (2010).

[20] R. F. Casten, Nucl. Phys. A **443**, 1 (1985).

[21] R. F. Casten, D. S. Brenner, and P. E. Haustein, Phys. Rev. Lett. **58**, 658 (1987).

[22] R. F. Casten, *Nuclear Structure from a Simple Perspective* (Oxford University Press, New York, 2000).